7. ANKARA INTERNATIONAL AEROSPACE CONFERENCE **AIAC-2013-040**

11-13 September 2013 - METU, Ankara TURKEY

DEVELOPMENT OF A NAVIER-STOKES SOLVER FOR HIGH-FIDELITY SIMULATION OF WIND TURBINE NOISE

Kenan CENGİZ* and Yusuf ÖZYÖRÜK†
Middle East Technical University
Ankara, Turkey

ABSTRACT

In this report, the first stage of the development process of a flow solver is presented. The solver is intended for high-fidelity simulation of wind turbine aeroacoustics. At this stage of the code development, compressible Euler solver, which has several discretization enhancements for convection term, is tested, validated and discussed. The enhancements include symmetry preservation of the discretized forms, fourth order accuracy and optimization for low-dispersion (DRP), all of which would be quite beneficial for low-level turbulence modeling and acoustic simulation problems where interference of possible numerical noise with small-scale eddies and high-frequency sound is not desired at all. The results show that the solver works at promised order of accuracy and exhibit good conservation properties, being a good start for the ultimate goal of successfully resolving turbulence and acoustic propagation.

INTRODUCTION

Public acceptance of wind turbines necessitates less noise emissions, which has been an issue for nearby residents since wind farms and residential areas happened to coincide around the world. Determination of the noise sources and designs curing it has been a hot topic [Raman, 2010], particularly the aerodynamic-related noise sources are more intensely focused due to their significance. Numerical simulation is an indispensable tool to investigate the aerodynamic noise sources around a wind turbine blade, despite the withcoming challenge of resolving complex unsteady flow structures accurately in acceptable computation time spans [Arakawa et al., 2005]. The turbulent character of the flow is the basis of the broadband noise [Oerlemans et al., 2007], usually being the dominant source over blade-thickness noise, trailing-edge bluntness noise etc., particularly for larger wind turbines [Doolan et al., 2012]. Broad-band noise has been simulated in two main approaches: Reynolds-averaged Navier-Stokes (RANS) based turbulence modeling [Tadamasa and Zangeneh, 2011], large/detached eddy simulation (LES/DES) and direct numerical simulation (DNS) [Arakawa et al., 2005; Sezer-Uzol and Long, 2006]. DNS is the most general one among these. However, it is impracticable for general problems due to the need for a tremendous number of cells and too small time steps to resolve the whole spectrum and time scales. Nevertheless, in literature, applications of DNS appear, but usually limited to simple geometry, low Reynolds number flows like channel flow with periodic boundary conditions. On the other hand, RANS based solvers can be reliable in fully-attached flow cases. However, the inherent time-averaging procedure eliminates the unsteadiness in small scales of turbulence, which renders it inappropriate for simulation of flow noise generation problems most of the time. At that point, use of LES/DES serves well both for capturing broad range of spectrum at an acceptable cost, as long as accompanied by a acoustic analogy integration algorithm (ie. FW-H [Williams and Hawkings, 1969] as utilized by [Arakawa et al., 2005; Tadamasa and Zangeneh, 2011]) to compute propagation of noise at a far-field observer.

*Research Asistant in METU Aerospace Engineering Department, Email: kcengiz@ae.metu.edu.tr
†Prof. in METU Aerospace Engineering Department, Email: yusuf@ae.metu.edu.tr

There are commercial codes like Fluent [ANSYS] which include LES/DES and RANS modules. However, because of low-order discretization approach of such codes, direct simulation of noise requires either very fine meshes or the range of the predicted noise frequency must be limited to low values because of dispersion and dissipation errors involved. When high-order methods are used, such errors are lowered and the need for very fine meshes can be relaxed. Therefore, our aim is to develop a high-order finite volume code to solve the Navier-Stokes equations with LES/DES capability which will enable us to obtain turbulent vortical structures that are responsible for aeroacoustic noise generation around open-rotors. Specifically, a high-order code is being developed for solution of the Navier-Stokes equations with LES/DES capability on structured meshes for wind turbine blade noise predictions. The discretization method is based on the fourth-order finite volume approach of Kok [Kok, 2009]. In this paper, we describe the developed code briefly and then present some test simulation results of compressible Euler to validate the spatial discretization schemes on 2-D, prior to any attempt to implement turbulence modeling and any wind turbine rotary simulation on 3-D domains.

METHODOLOGY

Stable high-order numerical schemes with low dispersion are required in simulation of physical phenomena where the effects of turbulent structures are decisive, such as aeroacoustic source simulations. In regular finite volume forms, local conservation of mass, momentum and total energy is ensured while kinetic energy, internal energy and sound-velocity is not conserved by convection locally. In inviscid cases where no change of total enthalpy is expected, unphysical generation of kinetic energy (through numerical production) disrupts stability. Besides, in viscous cases the unphysical production or dissipation of kinetic energy could interfere turbulent subgrid-scale stresses [Kok, 2009], ruining huge amount of cpu-time spent for turbulence modeling and simulation. In literature, skew-symmetric forms of convective terms have been implemented for compressible or incompressible flows via finite difference formulations [Verstappen and Veldman, 2003; Morinishi, 2010]. They enhance stability and accuracy such that need for physical/artificial dissipation is eliminated unlike conventional central discretizations [Pirozzoli, 2011]. This is a valuable merit because of computational overhead and possible induced inaccuracies of artificial dissipation. For compressible flows, Kok [Kok, 2009] was able to locally conserve (by convection) mass, momentum and total energy without sacrificing conservation of kinetic energy, internal energy and sound velocity locally on curvilinear grids with fourth-order accuracy and low-dispersive discretization.

Following Kok's methodology, the Euler equations can be defined in a special form,

$$D_i\mathbf{\Phi} = \frac{d\rho_i\mathbf{\Phi_i}}{dt} + \nabla_i\mathbf{F} = 0 \tag{1}$$

where $\Phi_i = \begin{Bmatrix} 1 \\ u_i \\ v_i \\ w_i \\ E_i \end{Bmatrix}$, $\mathbf{F} = \begin{Bmatrix} \overline{\rho\mathbf{V}} \\ \overline{\rho\mathbf{V}}\bar{u} + \bar{p}\vec{i} \\ \overline{\rho\mathbf{V}}\bar{v} + \bar{p}\vec{j} \\ \overline{\rho\mathbf{V}}\bar{w} + \bar{p}\vec{k} \\ \overline{\rho\mathbf{V}}\widetilde{E} + \widetilde{p\mathbf{V}} \end{Bmatrix}$. Here, the following averagings are essentially used in the derivation of the skew-symmetric forms,

$$\bar{u}_f = \frac{1}{2}(u_{i,j,k} + u_{i+1,j,k}) \tag{2a}$$

$$\widetilde{uv}_f = \frac{1}{2}(u_{i,j,k}v_{i+1,j,k} + u_{i+1,j,k}v_{i,j,k}) \tag{2b}$$

defined on the face between cells $V_{i,j,k}$ and $V_{i+1,j,k}$ without loss of generality. Note here that for sake of symmetry preservation, density goes with velocity instead of ϕ in face average calculations. In this form, basically, since the quadratic forms (ϕ^2), physically meaning kinetic and internal energy, are also conserved together with the quantities (ϕ), a skew-symmetric operator K can be found:

$$D(\frac{1}{2}\phi^2) = \frac{1}{2}\phi D\phi + \frac{1}{2}\phi A\phi = \phi K\phi \qquad (= 0) \tag{3}$$

It is clear that D and $-A$ are adjoint operators, hence a symmetric operator can be defined such that $S = \frac{1}{2}(D - A)$, $D = K + S$ and $A = K - S$. Substitution of definitions of advection and divergence operators reveals that symmetric operator S is actually the continuity equation. Therefore, the divergence operator D is equivalent to both advection operator A and the skew-symmetric operator K, thanks to the symmetric operator $S\phi = \frac{1}{2}\left(\frac{\partial\rho}{\partial t} + \nabla\cdot(\rho\mathbf{u})\right)\phi$ being equal to zero.

Non-uniformity on grids does not disrupt symmetry unlike in finite difference approaches [Morinishi et al., 1998] because grid-dependant averaging weights are not necessary to maintain accuracy. Furthermore, grid metrics are imposed as face area vectors and volumes of the cells of the finite volumes (See Figure 1), preserving symmetry as well.

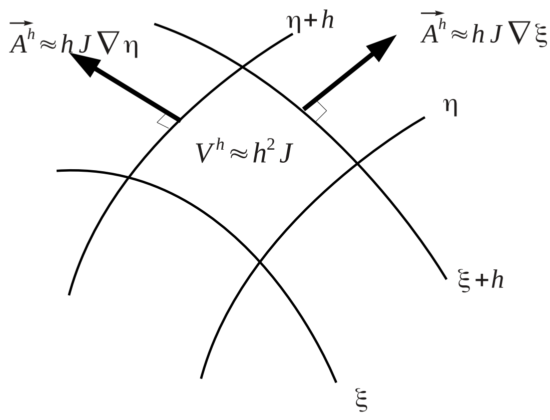

Figure 1: Metrics of a cell on a curvilinear 2-D grid

Fourth-order accuracy can be achieved through use of a larger cell. Flux computations are simply done in the same manner on the grid, but with $3h$ cell size. Afterwards, the leading error term of the second-order scheme is cancelled via Richardson extrapolation [Verstappen and Veldman, 2003]. Eventually, the fourth-order accurate gradient operator is nothing but a linear combination of the two second-order operators. Thus, the flux balance and volume discretization is found as,

$$B_i^{4th} = \frac{9}{8}B_i^h - \frac{1}{8\cdot 3^d}B_i^{3h} \tag{4a}$$

$$V_i^{4th} = \frac{9}{8}V_i^h - \frac{1}{8\cdot 3^d}V_i^{3h} \tag{4b}$$

Dispersion-relation preserving methodology can be devised in the same manner. Another larger cell would act as an extra degree of freedom resembling the extra points for DRP in finite difference stencils [Tam and Webb, 1993]. Here, since the finite volume description is cell-centered, a cell with $2h$ size has corners falling on neighbouring cell centers (see Figure 2). Note that to maintain fourth-order accuracy, a fourth-order is necessary for the metrics on the cell-centers. The fourth-order DRP discretization turns out to be a linear combination of $h, 2h$ and $3h$ cell-sized second-order discretizations of volume and flux,

$$B_i^{DRP} = \beta\left(\frac{4}{3}B_i^h - \frac{1}{3\cdot 2^d}B_i^{2h}\right) + (1-\beta)\left(\frac{9}{8}B_i^h - \frac{1}{8\cdot 3^d}B_i^{3h}\right) \tag{5a}$$

$$V_i^{DRP} = \beta\left(\frac{4}{3}V_i^h - \frac{1}{3\cdot 2^d}V_i^{2h}\right) + (1-\beta)\left(\frac{9}{8}V_i^h - \frac{1}{8\cdot 3^d}V_i^{3h}\right) \tag{5b}$$

where d is the dimension of the problem. Here, taking $\beta = 0$ brings back the basic fourth-order discretization. In fact, it is the reserved parameter for optimization to achieve Tam&Webb's DRP discretization for finite difference methods. On uniform cartesian grid, since FVM and central FDM discretizations turns out to be equivalent discretized equations, a choice of $\beta = 2.00047085298$ matches the FVM to low-dispersion optimized scheme of Tam&Webb.

Time marching procedure is chosen to be the efficient four-stage Runge-Kutta scheme [Jameson, 1985] with fourth-order accuracy (for linear problems) and good stability behaviour.

RESULTS

The inherent spatial discretizations are intented to be validated via an isentropic vortex convection test problem, whose analytical solution is simply transport of the initial vortex as it is. Cartesian mesh sizes of 100×100,

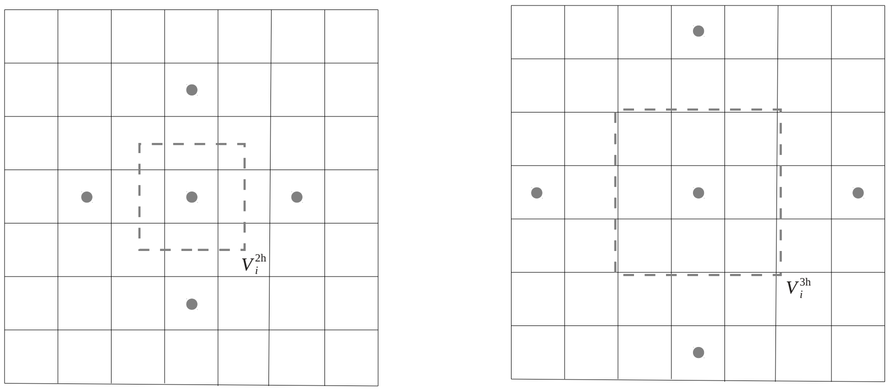

(a) Control volume with $2h$ size for use in DRP. (b) Control volume with $3h$ size for fourth-order accuracy.

Figure 2: Control volumes used apart from regular cell-based V_i^h

200×200 and 400×400 are generated with some non-uniformity (Figure 3). The mesh is generated via smooth transformation of uniform mesh. A strong vortex ($u_A/V_\infty = 0.8$) is convected under $M_\infty = 0.5$ for a time period of $V_\infty t/L = 30$ and periodic conditions on the boundaries. The inital form of the solution is given by,

$$\mathbf{V} = \begin{Bmatrix} V_\infty \\ 0 \\ 0 \end{Bmatrix} + u_A e^{(1-(r/b)^2)/2} \begin{Bmatrix} (y-y_0)/b \\ -(x-x_0)/b \\ 0 \end{Bmatrix} \tag{6}$$

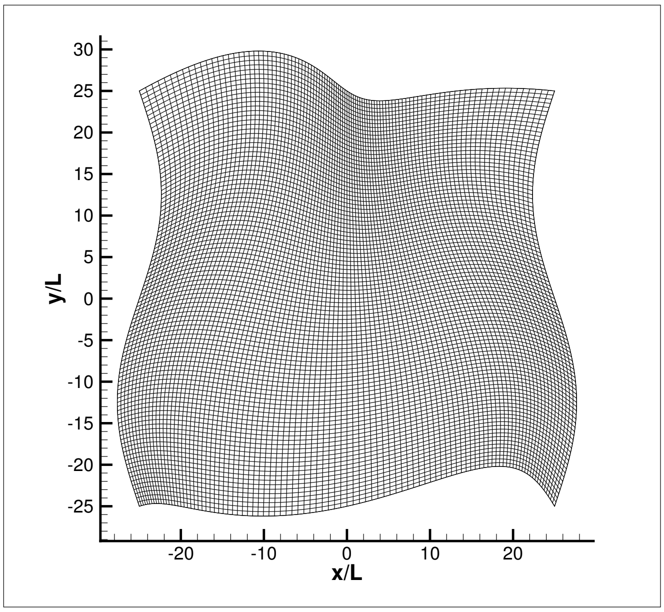

Figure 3: Non-uniform cartesian mesh

for a 2-D vortex defined on $[-25L, 25L]^2$. r is the distance from the vortex center (x_0, y_0). A representative length scale for the vortex can be defined from $e^{-(r/b)^2} = \frac{1}{2}$ at $r = L$. The primitive variables can be found using isentropic relations,

$$\frac{T}{T_\infty} = \left(\frac{p}{p_\infty}\right)^{(\gamma-1)/\gamma} = \left(\frac{\rho}{\rho_\infty}\right)^{\gamma-1} = 1 - \frac{\gamma-1}{2}\frac{u_A^2}{c_\infty^2} e^{1-(r/b)^2} \tag{7}$$

A fourth-order efficient four-stage Runge-Kutta time integration is used. Since the compact RK4 is second-order accurate for nonlinear equations, a non-dimensional time step size of order spatial step-size squared in transformed coordinates ($u_\infty \Delta t/L \sim \Delta x^2$) or one order higher than that when instability shows up ($u_\infty \Delta t/L \sim \Delta x^3$), is chosen to prevent the time integration error from overshadowing the spatial discretization error. The vortex is convected a distance from $-15L$ to $15L$ in the x-direction. See the temperature contours in Figure 4, of the vortex on the 100×100 mesh. Observe the loss of shape and position with some of the schemes. Using central schemes with symmetry preservation is known to lower numerical dissipation, hence reduces peak amplitude loss. It can be observed that the non-symmetric form of divergence does not preserve the peak of the vortex as compared to symmetric form with same accuracy order. Morever, since dispersion cause waves to travel at different speeds, loss of position and shape of the vortex is minimized with low-dispersion DRP scheme (Figure 4(e)). As expected, position and shape of the vortex is most immensely preserved with fourth-order DRP scheme on 400×400 mesh (Figure 4(f)).

The symmetry-preserving scheme proved to be stable without any means of artificial dissipation for this problem. The skew-symmetric form owes this to local and global conservation of total energy by convection, avoiding spurious generation of kinetic and internal energies. However, for compressible flows, where density can drop to some extent, unbounded increase of velocity is not avoided in global conservation of total energy. Still, stability is dramatically enhanced, even though, to eliminate small-amplitude oscillations, a minimal artificial diffusion may be required in other problems such as problems with submerged bodies. In contrast, a standard scheme ($\mathbf{F} = \overline{\rho \mathbf{V} \phi}$) without artificial diffusion would be unstable giving no results at all. Hence, results of the standard scheme are obtained by help of an artificial diffusion, whereas the Jameson-type averaging Jameson [1983] ($\mathbf{F} = \overline{\rho \mathbf{V}}\, \overline{\rho \phi}/\overline{\rho}$), which slightly differs from the skew-symmetric form Kok [2009], did not require one for this test problem.

An error analysis is also performed in order to validate the accuracy orders of the schemes. Figure 5 shows logarithmic plots of the root-mean-squared error values with respect to doubling mesh sizes. The skew-symmetric fourth-order DRP scheme exhibits the lowest error for all variables. The promised order of accuracies of the schemes seem to be maintained. As to u, v and T, the non-symmetric schemes proved to be almost equally accurate with their symmetric counter-parts, except the standard scheme has little more error due to the influence of artificial diffusion. However, entropy generation levels (Figure 5(d)) plot another story: All schemes demonstrate their success with different levels of error. Entropy generation has to be solely related to numerical dissipation for this inviscid problem (no heat generation/conduction, no shocks). Hence, it can be taken as a measure of numerical dissipation. The skew-symmetric scheme proved to cause less dissipation error, in fact, one order and two order less than corresponding Jameson-type and standard schemes, respectively. The standard scheme has the largest error, due to the fact that an extra dissipation (artificial diffusion) is essentially added. Observe the entropy error results of fourth-order DRP schemes, where minimization of dispersion error for each case provides one order less error. Eventually, Figure 5(d) can be deemed a splendid illustration of merits of skew-symmetry as well as DRP feature of discretizations.

Essentially, the skew-symmetric discretization of convection term requires additional computations (see Section) to obtain averaged flux on cell faces. This results in more CPU time for a simulation of same accuracy order on the same mesh. For instance, the standard scheme costs 1.3 multiple of the Jameson-type scheme does, whereas the skew-symmetric scheme costs 1.8 times what the Jameson-type scheme does. It is not a big trouble as the profit made from mesh size is considered. In fact, it is observed from the results of the aforementioned vortex problem that the low-dispersion fourth-order skew-symmetric scheme on 200×200 mesh attains the accuracy obtained with the low-dispersion Jameson-type basic scheme on 400×400 mesh. Accordingly, the skew-symmetric form performs around 2.7 times faster than the basic form to achieve the same accuracy, thanks to the mesh-size related cost reduction. The performance gap further extends as second-order basic scheme is compared, and even further on 3-D domains.

CONCLUSION

In this work, first development report of a solver intended for wind turbine high-fidelity aeroacoustic simulation is presented. The symmetry-preserving qualities of the convection term proved to be quite beneficial at this very first stage of the flow solver development process, where viscosity is excluded. There does exist some cpu overhead that comes with the implemention of symmetry preservation, compared to traditional discretization schemes. However, it was claimed that [Verstappen and Veldman, 2003] for a given accuracy, the fourth-order symmetry-preserving scheme requires approximately three times larger grid size than that required by a traditional Lagrangian discretization method of same order of accuracy. In this work as well, the fourth-order symmetry-preserving scheme proved to be 2.7 times faster than the basic scheme of same accuracy, with half the mesh size. Furthermore, the cpu time saved in the problems that do not necessiate artificial dissipation for the present scheme, is another plus compared to traditional schemes, because of the fact that artificial dissipation computation is a considerable amount of work on cpu at each step of iterations, not to mention the introduction of extra inaccuracy to the solution.

Acknowledgement

Funding by TÜBİTAK (the Scientific and Technological Research Council of Turkey) is gratefully acknowledged under 1001 programme (grant no.112M106).

References

ANSYS. Fluent flow solver software. URL http://www.ansys.com.

Chuichi Arakawa, Oliver Fleig, Makoto Iida, and Masakazu Shimooka. Numerical Approach for Noise Reduction of Wind Turbine Blade Tip with Earth Simulator. *Earth*, 2(March):11–33, 2005.

Con Doolan, Danielle J Moreau, and Laura A Brooks. Wind turbine noise mechanisms and some concepts for its control. *Acoustics Australia*, 40(1):7–13, 2012.

A Jameson. Numerical solutions of the euler equations for compressible inviscid flows. *Princeton University, MAE Report*, 1643, 1983.

Antony Jameson. Numerical solution of the euler equations for compressible inviscid fluids. *Numerical methods for the Euler equations of Fluid Dynamics*, 1, 1985.

J.C. Kok. A high-order low-dispersion symmetry-preserving finite-volume method for compressible flow on curvilinear grids. *Journal of Computational Physics*, 228(18):6811–6832, October 2009.

Y. Morinishi, T.S. Lund, O.V. Vasilyev, and P. Moin. Fully Conservative Higher Order Finite Difference Schemes for Incompressible Flow. *Journal of Computational Physics*, 143(1):90–124, June 1998.

Yohei Morinishi. Skew-symmetric form of convective terms and fully conservative finite difference schemes for variable density low-Mach number flows. *Journal of Computational Physics*, 229(2):276–300, January 2010.

S Oerlemans, P Sijtsma, and B Mendezlopez. Location and quantification of noise sources on a wind turbine. *Journal of Sound and Vibration*, 299(4-5):869–883, 2007.

Sergio Pirozzoli. Stabilized non-dissipative approximations of Euler equations in generalized curvilinear coordinates. *Journal of Computational Physics*, 230(8):2997–3014, April 2011.

G. Raman. Wind turbines: clean, renewable and quiet? *Noise Notes*, 9(1):35–44, 2010.

Nilay Sezer-Uzol and Lyle N Long. 3-d time-accurate cfd simulations of wind turbine rotor flow fields. *AIAA paper*, 394:2006, 2006.

A Tadamasa and M Zangeneh. Numerical prediction of wind turbine noise. *Renewable Energy*, 36(7):1902–1912, 2011.

Christopher KW Tam and Jay C Webb. Dispersion-relation-preserving finite difference schemes for computational acoustics. *Journal of computational physics*, 107(2):262–281, 1993.

R.W.C.P. Verstappen and A.E.P. Veldman. Symmetry-preserving discretization of turbulent flow. *Journal of Computational Physics*, 187(1):343–368, May 2003.

JE Ffowcs Williams and David L Hawkings. Sound generation by turbulence and surfaces in arbitrary motion. *Philosophical Transactions of the Royal Society of London. Series A, Mathematical and Physical Sciences*, 264(1151):321–342, 1969.

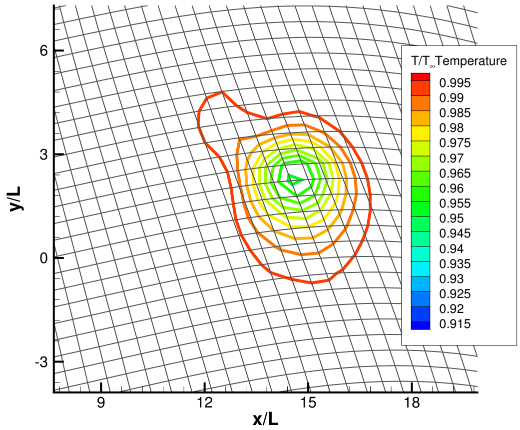

(a) Second-order scheme conserving skew-symmetry on 100×100 grid

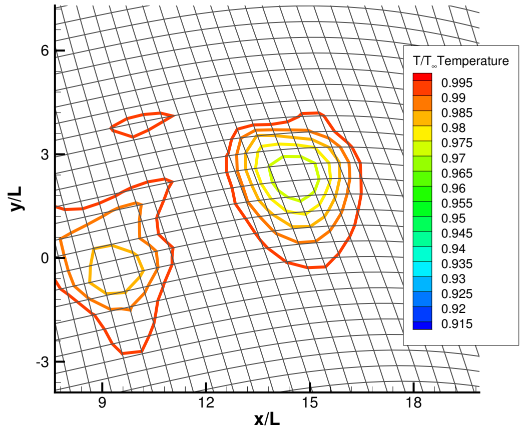

(b) Second-order scheme (Jameson-type scheme) on 100×100 grid

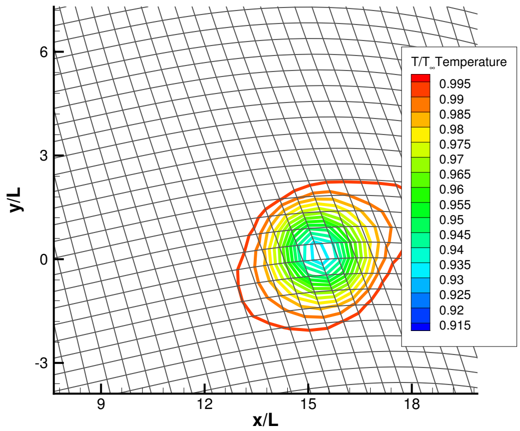

(c) Fourth-order scheme conserving skew-symmetry on 100×100 grid

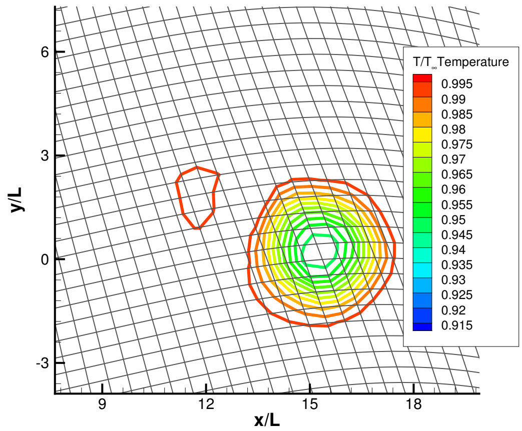

(d) Fourth-order scheme (Jameson-type scheme) on 100×100 grid

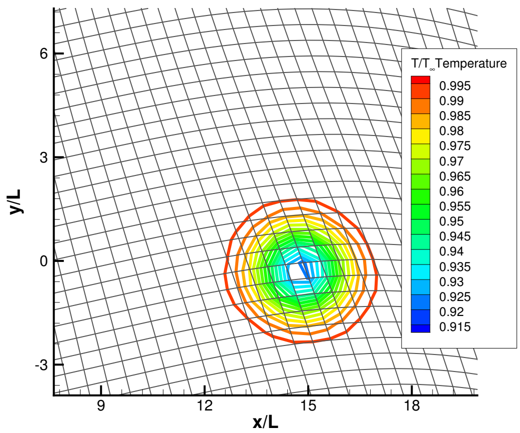

(e) Fourth-order DRP scheme conserving skew-symmetry on 100×100 grid

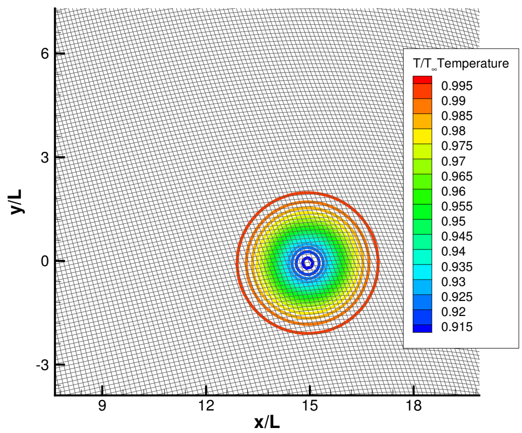

(f) Fourth-order DRP skew-symmetric scheme on 400×400 grid

Figure 4: Temperature contour of the isentropic vortex using symmetry-preserving and Jameson-type schemes

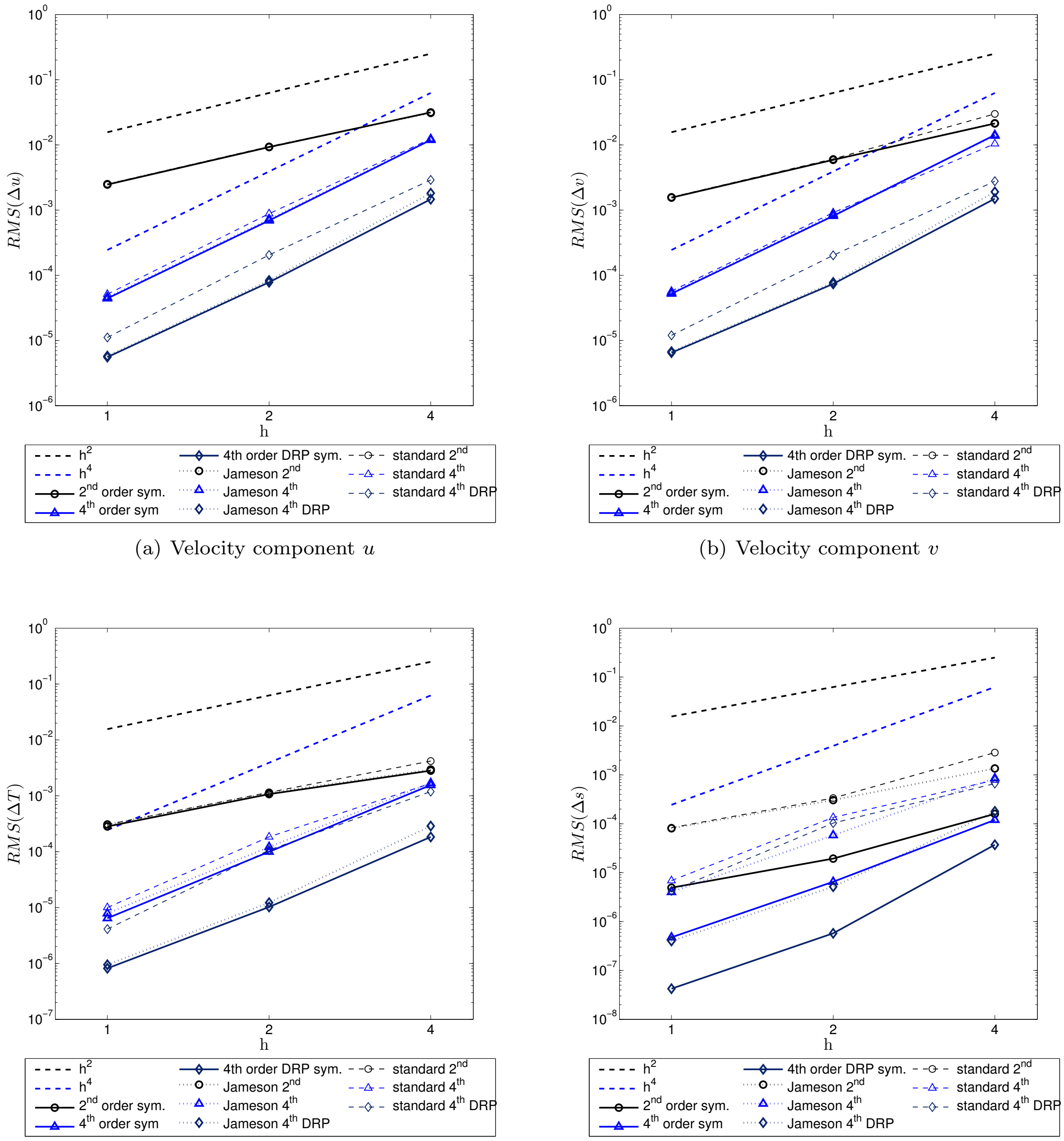

(a) Velocity component u

(b) Velocity component v

(c) Temperature

(d) Entropy

Figure 5: Step-size vs. root-mean-square of differences of isentropic vortex convection solutions from analytical values of nondimensional velocities u and v, temperature, entropy.